

# An Electronically Controlled Leaky-wave Antenna Based on Corrugated SIW Structure with Fixed-Frequency Beam Scanning

Ke Chen, Y. H. Zhang, S. Y. He, H. T. Chen, and G. Q. Zhu

**Abstract**—A novel electronically controlled (EC) leaky-wave antenna (LWA) based on corrugated substrate integrated waveguide (CSIW) with fixed-frequency beam-steerable capability is presented in this letter. This structure is based on a CSIW structure with rectangular ring slots and metallic vias to the ground, which realizes two isolated DC equipotential planes. Each slot of the rectangular ring is loaded with a varactor diode, and thus the series and shunt capacitance are tunable by adjusting the DC bias voltage, which eventually results in beam scanning at a fixed frequency. The proposed antenna is a single-layer structure and has a simplified DC bias network, which merely needs an inductor and a short microstrip line. An electronically controlled beam-steerable CSIW LWA is designed and experimentally validated. It is experimentally demonstrated that the radiation angle ranges from  $-40.66^\circ$  to  $31.32^\circ$  as the bias voltage is tuned from 32 V to 7.5 V at 4.5 GHz.

**Index Terms**—Fixed-frequency beam-steerable, corrugated substrate integrated waveguide, leaky wave antenna.

## I. INTRODUCTION

PLANAR LEAKY-WAVE antennas (LWAs) have attracted much attention in wireless communication systems due to their low-profile, frequency-scanning capability and ease of feeding [1]. However, the main beam of conventional LWAs can only scan in the forward quadrant or backward quadrant. Quasi-uniform and -1-order mode LWAs are proposed to obtain continuous beam scanning from backward to forward [2], [3].

Recently, LWAs based on substrate integrated waveguide (SIW) have raised significant research attention due to low loss, high-power capacity and ease of fabrication [3], [4]. Furthermore, SIW, half-mode SIW (HMSIW), HMSIW with spoof surface plasmon polariton (SSPP) and corrugated SIW (CSIW) structures are applied to realize LWAs with frequency scanning capability [4]–[8]. Compared to the HMSIW and HMSIW-SSPP structure, the CSIW structure without metallic vias to the ground, which makes have the potential to design a simplified DC bias network.

However, frequency-dependent LWAs have suffered a limitation because most modern wireless communication

systems operate in a fixed frequency band. Fixed-frequency beam-steerable can be achieved by using p-i-n diodes as switches to control phase shift, but it is limited to several discrete radiation angles [9]. Continuous beam scanning controlled LWAs have been achieved by co-planar waveguide based continuous transverse stub structure or Fabry-Pérot structure [10], [11], but those antennas need a high profile. Backward to forward scanning electronically controlled LWA has been obtained in composite right/left-handed transmission line transmission line (CRLH-TL) loaded with varactor diodes [12]. A circularly polarized LWA based on CRLH-TL structure with square-shaped patch is presented in [13]. However, the radiation efficiency is not high due to the loss of microstrip (MS) structure, and the DC bias network is quite complex. To obtain fixed-frequency beam-steerable with high radiation efficiency, some HMSIW based LWAs have been designed [14], [15]. However, the LWA in [14] is not able to realize electronically control due to no DC bias network. Furthermore, the LWA in [15] relies on multilayer substrates and complex DC bias network, which is hard to fabricate. In order to overcome those drawbacks, a novel LWA based on CSIW structure with the advantage of ease to fabricate is proposed [8].

In this letter, a beam tunable leaky-wave antenna based on corrugated substrate integrated waveguide at a fixed frequency is proposed. By introducing rectangular ring slots and metallic vias on CSIW structure, two isolated DC equipotential planes on a single-layer are obtained. Each rectangular ring slot is loaded with four varactor diodes, and thus the series and shunt capacitance are tunable by changing the DC bias voltage, which eventually results in beam scanning at a fixed frequency. The proposed LWA is easy to fabricate owing to its single-layer structure and extremely simplified DC bias network.

The proposed antenna structure and analysis are described in detail in Section II. Full-wave analysis and the measured results are shown in Section III. Finally, a conclusion is drawn in Section IV.

## II. ANTENNA DESIGN AND ANALYSIS

The CSIW structure is using quarter-wave open-circuit microstrip stubs in place of metallic vias to offer electric sidewalls. So the CSIW structure confines energy transmission in the same manner as that of the SIW. The method to calculate the equivalent width of CSIW structure can be simplified as a dielectric-filled waveguide similar to SIW [16]. Besides, the length of microstrip open-circuit stubs is quarter wavelength at the center frequency. It should be noted that the propagation

Manuscript received October 20, 2018. This work was supported by the National Nature Science Foundation of China under Grant 61301061. (Corresponding author: Yunhua Zhang.)

K. Chen, Y. H. Zhang, S. Y. He, and G. Q. Zhu are with the School of Electronic Information, Wuhan University, Wuhan, 430072, China (e-mail: 2013202120030@whu.edu.cn; zhangyunhua@whu.edu.cn).

H. T. Chen is with the Wuhan Maritime Communication Research Institute, Wuhan, 430079, China.

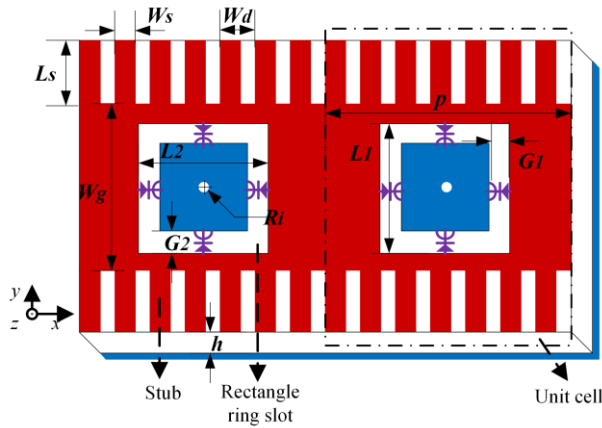


Fig. 1. Scheme of the proposed CSIW based unit cell.  $L_s = 15$  mm,  $W_g = 30$  mm,  $W_s = 1$  mm,  $W_d = 2$  mm,  $L_1 = 18$  mm,  $L_2 = 10.5$  mm,  $G_1 = 0.8$  mm,  $G_2 = 0.8$  mm,  $R_i = 0.3$  mm,  $p = 20$  mm,  $h = 1$  mm,  $\epsilon_r = 3.55$ .

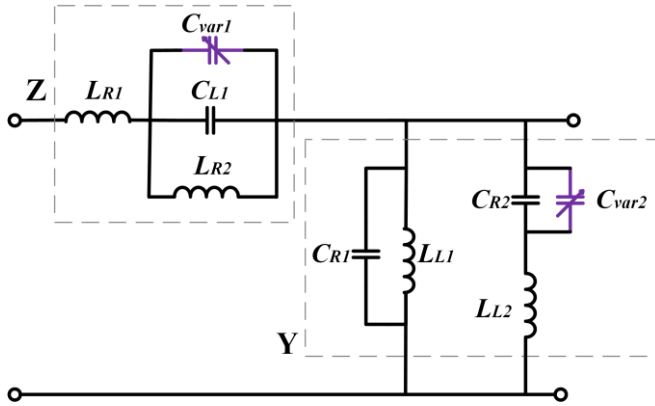


Fig. 2. Equivalent circuit of unit cell.

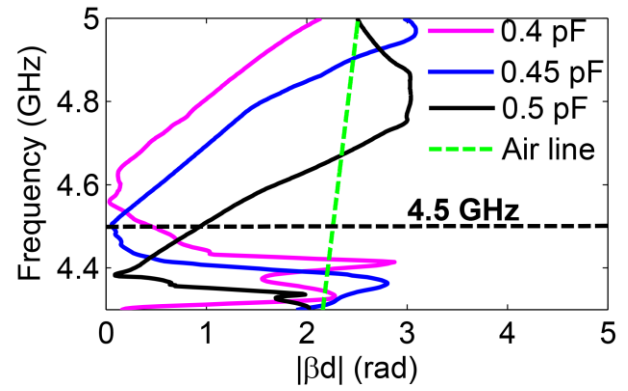
mode is quasi-TEM mode when the microstrip open-circuit stub is much less than the quarter wavelength [17].

Fig. 1 shows the scheme of the proposed LWA based on CSIW structure. The unit cell includes four varactors and a CSIW structure with a rectangular ring slot. By implemented rectangular ring slots and metallic vias on the top plane, two isolated DC equipotential planes on a single-layer are obtained. Four varactor diodes are loaded on each rectangular ring slot, and the series and shunt capacitor of varactors are tunable by adjusting the DC bias voltage. Moreover, the red color is one DC equipotential plane used for DC bias, and the blue color for the ground plane. So the DC bias network will be extremely simplified.

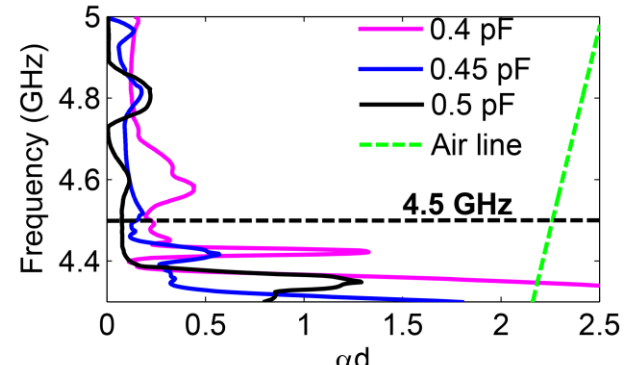
In order to realize the beam scanning of LWA from backward to forward at principal mode, the proposed CSIW structure must possess propagation characteristic similar to CRLH-TL structure. So the proposed antenna should operate near or below the cutoff frequency of the main waveguide to obtain the left-handed propagation behavior [2]. And the radiation angle of quasi uniform LWA can be calculated as:

$$\theta = \sin^{-1}(\beta/k_0) \quad (1)$$

where  $\beta$  is the phase constant and  $k_0$  is the propagation constant



(a)



(b)

Fig. 3. Complex propagation constant of the proposed LWA unit cell at  $C_{var0} = 0.4$  pF,  $0.45$  pF,  $0.5$  pF. (a) Phase constant. (b) Attenuation constant.

of free space. When  $\beta < k_0$ , the proposed structure is in fast wave region and the mode from guide wave mode to leak wave.

The equivalent circuit model of unit cell structure is obtained as shown in Fig. 2, which consists of series impedance  $Z$  and shunt admittance  $Y$ . Here, varactor diodes are simplified as a capacitor adjusted by reverse voltage. And the propagation constant can be calculated as follows [2]:

$$\beta p = \cos^{-1}(1 + Z(V)Y(V)) \quad (2)$$

where the series impedance  $Z$  includes series capacitor and series inductor. The rectangular ring slots and the two series varactors offer the series capacitor  $C_{L1}$  and  $C_{var1}$ , while the patch of top plane provides the equivalent series inductor  $L_{R1}$  and  $L_{R2}$ . Similarly, shunt capacitor and shunt inductor make up the shunt admittance  $Y$ . The patch of top plane, the rectangular ring slots, and the two shunt varactors offer shunt capacitor  $C_{R1}$ ,  $C_{R2}$ , and  $C_{var2}$ . And the metallic vias and open-circuit stubs provide the shunt inductor  $L_{L1}$  and  $L_{L2}$ . By changing the reverse voltage, the series and shunt capacitance of varactors can be adjusted, and then the  $\beta$  becomes tunable by the reverse voltage.

The primary zero points of  $Z$  and  $Y$  can be written as follows:

$$\omega_{se} = \frac{1}{C_{L1} + C_{var1}} \left( \frac{1}{L_{R1}} + \frac{1}{L_{R2}} \right) \quad (3)$$

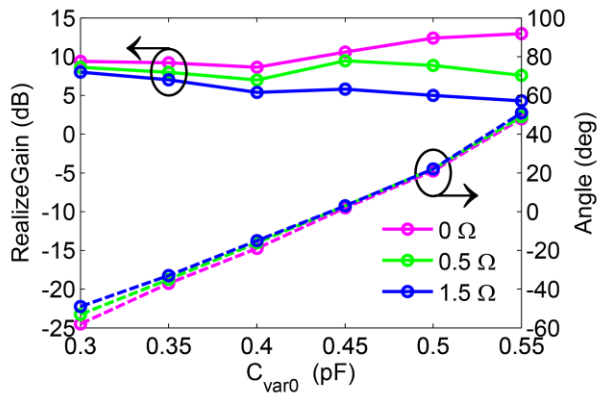


Fig. 4. Simulated gain (solid lines) and angle (dashed lines) for different values of internal resistance  $R_s$  of the varactor diode.

$$\omega_{sh} = \frac{1}{L_{L1}(C_{R1} + C_{R2} + C_{var2})} \quad (4)$$

where those equivalent circuit parameters can be extracted from simulated S-parameters.  $C_{var1} = C_{var0}/2$  and  $C_{var2} = 2C_{var0}$ , meanwhile  $C_{var0}$  is the capacitance of the varactor diode. When the  $C_{var0}$  increases, the  $\omega_{se}$  and the  $\omega_{sh}$  will decrease simultaneously. At a fixed frequency  $\omega_0$ , the balanced frequency  $\omega_b = \sqrt{\omega_{se}\omega_{sh}}$  can be lower than, equal to or higher than the  $\omega_0$  by changing the values of  $C_{var0}$ . Thus the value of  $\beta$  from negative, to zero, then to positive at a fixed frequency is achieved. It is noteworthy that short-open calibration can be employed to eliminate the high-order mode effects and port discontinuities, thus obtaining accurately complex propagation constants [17].

In Fig. 3, the propagation constants are plotted at  $C_{var0} = 0.4$  pF, 0.45 pF and 0.5 pF. From Fig. 3(a), backward and wave propagation can be obtained over 4.4-4.55 GHz and 4.4-4.7 GHz when the  $C_{var0}$  values are 0.4 and 0.5 pF, respectively. And  $\beta = 0$  at 4.5 GHz is achieved when the  $C_{var0}$  is 0.45 pF. So the radiation angle from forward, broadside or backward at 4.5 GHz is achieved by changing the value of  $C_{var0}$ . At 4.5 GHz, the attenuation constant of backward-wave is larger than forward-wave, as shown in Fig. 3(b). The propagation constant has some fluctuations at low frequency region for this structure is near the cutoff frequency of the CSIW and still exist a narrow open-stopband.

### III. SIMULATED AND MEASURED RESULTS

#### A. Simulation Analysis

In order to satisfy the capacitance range in Section II, SMV1430-079LF varactor diodes are used in the design of CSIW based EC LWA, and  $C_{var0}$  varies in the range of 0.3 pF-0.55 pF. It is noted that the internal resistance  $R_s$  of each varactor is a bit large and about 1.5  $\Omega$ .

Then, the ten cells cascaded EC LWA based on CSIW structure with different values of internal resistance  $R_s$  is simulated, as shown in Fig. 4. When  $R_s = 0$ , the simulated realized gains are better than 8.6 dB, and the maximum gain is 12.8 dB. Meanwhile, the beam scanning is at least from  $-58^\circ$  to

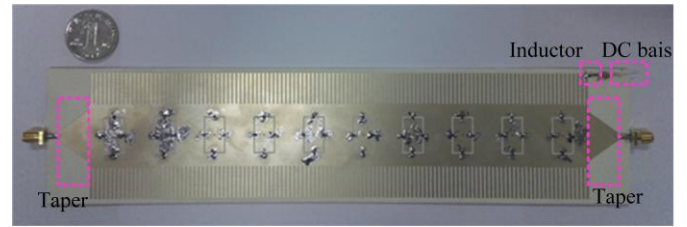


Fig. 5. Photograph of the fabricated EC CSIW LWA.

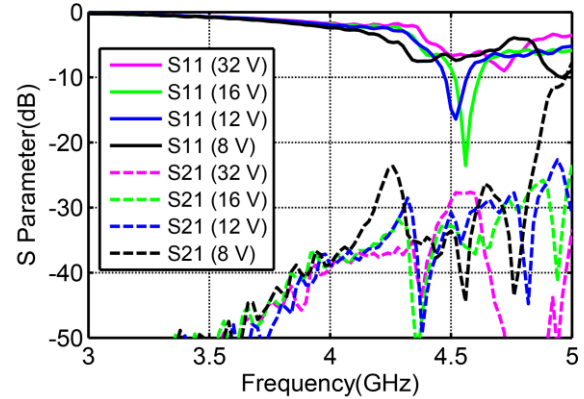


Fig. 6. Measured S-Parameters at different reverse bias voltages  $V = 32$  V, 16 V, 12 V and 8 V.

$48^\circ$  as the  $C_{var0}$  from 0.3 pF to 0.55 pF. In addition, the total efficiencies of antenna are 0.78, 0.92, and 0.76 when the  $C_{var0}$  are 0.5, 0.44, and 0.32 pF, respectively. With the  $R_s$  increasing from 0  $\Omega$  to 1.5  $\Omega$ , the realized gains of the backward radiation region have a bit decrease and the realized gains of the forward radiation region decrease rapidly. The reason for this is the attenuation constant of backward radiation region is larger than forward radiation. And the beam angles are staying almost the same when the  $R_s$  changes from 0  $\Omega$  to 1.5  $\Omega$ . It is demonstrated that the realized gain of the proposed antenna can be significantly influenced by the ohmic losses of varactors.

#### B. Experimental Results

For verification, an EC CSIW LWA cascaded by ten unit cells is fabricated, as shown in Fig. 5. The fabricated antenna is a single-layer substrate and has a simplified DC bias network, which merely needs an inductor, a short microstrip line. The antenna prototype is manufactured by Rogers 4003c substrate ( $\epsilon_r = 3.55$ ), and the whole size is 240 mm  $\times$  60 mm  $\times$  1 mm. Skyworks SMV1430-079LF varactor diodes are utilized to implement unit cells structure, and Murata chip inductor with 20 nH is used for DC bias. The internal resistance  $R_s$  of each varactor is about 1.5  $\Omega$ . A tapered microstrip line is employed to feed the proposed antenna for impedance match [18].

The measured S-parameters are shown in Fig. 6. According to Fig. 6,  $S_{21}$  is almost below -25 dB at 4.5 GHz due to the ohmic losses of varactors. Meanwhile  $S_{11}$  is -14.9, -9.1, -7.0, and -6.7 dB at the bias voltage is 8 V, 12 V, 16 V, and 32 V, respectively. The difficulty of matching to the conventional 50  $\Omega$  transmission line for the backward scanning cases is due to the large bloch impedance. By optimizing the tapered microstrip line, the better impedance match could be obtained.

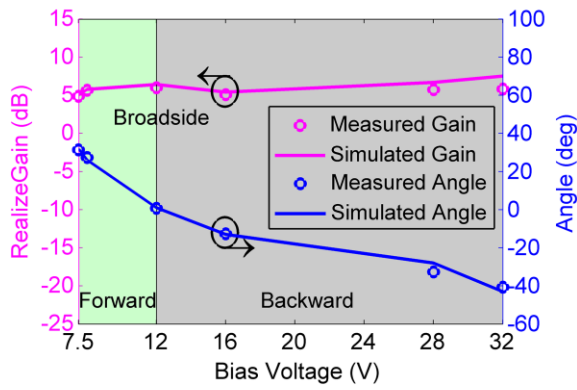


Fig. 7. Realized gain and beam angle of the proposed antenna at 4.5 GHz as bias voltage changes (both simulated and measured).

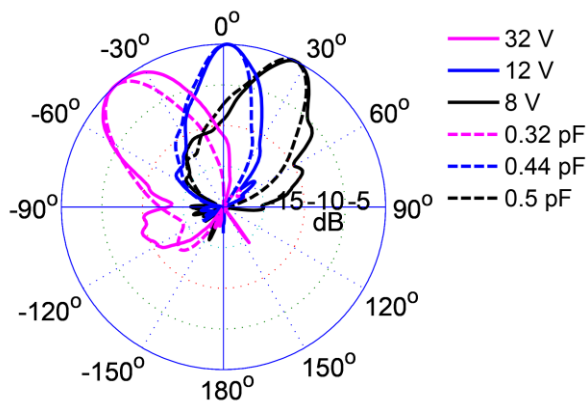


Fig. 8. Measured and simulated radiation patterns in the E-plane at 4.5 GHz. The measurement results are solid line and the simulation results are dashed line.

The comparison between the measured and simulated results of realized gain and beam angle as shown in Fig. 7. It is shown that, at 4.5 GHz, the measured results of radiation angles are in good agreement with the simulated results at all bias voltages. And the radiation angle is  $31.32^\circ$ ,  $27.3^\circ$ ,  $0.68^\circ$ ,  $-12.7^\circ$ ,  $-32.65^\circ$  and  $-40.66^\circ$  at the different reverse voltages 7.5, 8, 12, 16, 28, and 32 V, respectively. The radiation angle is scanning from forward to backward as the bias voltage increases. The measured results of antenna gain are about 1 dB lower than the simulated results in some regions, which is due to the dimensional tolerance and material loss. And the measured results of realized gain are 4.9, 5.6, 6, 5.1, 5.7 and 5.8 dB at the different reverse voltages 7.5, 8, 12, 16, 28, and 32 V, respectively. The measured results demonstrate that the beam scans from  $-40.66^\circ$  to  $31.32^\circ$  as the bias voltage increases from 7.5 V to 32 V with broadside radiation at 12 V, and the measured results of gain are almost better than 5 dB.

The measured and simulated normalized radiation patterns of E-plane at 4.5 GHz are depicted in Fig. 8, showing a good agreement. The measured beamwidth of backward radiation is slightly broaden than simulated beamwidth, which is due to the loss the dimensional tolerance and the capacitance shift of varactors. And the measured efficiencies of antenna are 0.17,

TABLE I

Performance Comparison of Different Continuous Fixed-Frequency Beam-Steerable LWAs

|                      | [10]               | [12]               | [13]               | This work          |
|----------------------|--------------------|--------------------|--------------------|--------------------|
| Operate frequency    | 2.4 GHz            | 3.3 GHz            | 2.4 GHz            | 4.5 GHz            |
| Range                | $58\sim 124^\circ$ | $-49\sim 50^\circ$ | $-17\sim 40^\circ$ | $-41\sim 31^\circ$ |
| Range (Gain>5dB)     | $58\sim 124^\circ$ | $-49\sim 14^\circ$ | $-7\sim 15^\circ$  | $-41\sim 31^\circ$ |
| Average Gain         | 9.7 dBi            | 6 dBi              | 4.9 dBi            | 5.6 dBi            |
| Max EFF              | 0.39               | N/A                | 0.22               | 0.28               |
| Number of diodes     | Fixed capacitor    | 90                 | 60                 | 40                 |
| Size ( $\lambda_0$ ) | 0.5                | 2.2                | 3.25               | 3.6                |
| Height               | 30 mm              | 1.6 mm             | 1 mm               | 1 mm               |
| Technology           | CPW-C TS           | MS                 | MS                 | CSIW               |

0.26, and 0.28 at the different reverse voltages 7.5, 12, and 32 V, respectively. Due to the ohmic losses of varactors and material loss, the measured efficiencies are much lower than simulated efficiencies.

Finally, in Table I, performance of the proposed antenna is compared to other recently continuous fixed-frequency beam-steerable LWAs [10], [12], and [13], where EFF is the efficiency of antenna. Compare to [10], the proposed antenna is an electronically controlled antenna and have a low profile. It is noted that the fixed-capacitor application has a relatively high gain due to the low ohmic losses of fixed-capacitor. The proposed antenna shows comparatively better performance and uses less number of varactor diodes compare with other electronically controlled applications. In addition, the proposed antenna is much easier to fabrication than other electronically controlled LWAs with continuous beam-steerable due to the single-layer structure and extremely simplified DC bias network.

#### IV. CONCLUSION

An electronically controlled leaky-wave antenna based on a corrugated substrate integrated waveguide with single-layer structure and extremely simplified DC bias network has been presented in this letter. Full-wave analysis of the proposed antenna shows that the radiation angle is from  $-58^\circ$  to  $48^\circ$  when the capacitance from 0.3 pF to 0.55 pF at a fixed frequency. This antenna has been fabricated with varactor diodes loading and the fixed frequency beam scanning capability has been experimentally validated. By adjusting reverse bias voltage from 32 V to 7.5 V, the beam scans from  $-40.66^\circ$  to  $31.32^\circ$  continuously, and the gains are almost better than 5 dB. The proposed LWA achieves a wide beam steering range about  $72^\circ$ . Finally, using varactor diodes with low ohmic losses can improve the antenna performance effectively.



# REFERENCES

- [1] A. A. Oliner and D. R. Jackson, *Antenna Engineering Hand Book*. 4th ed. New York, NY, USA: McGraw-Hill, 2007.
- [2] D. R. Jackson, C. Caloz, and T. Itoh, "Leaky-wave antennas," *Proc. IEEE*, vol. 100, no. 7, pp. 2194–2206, Jul. 2012.
- [3] F. Xu and K. Wu, "Understanding Leaky-Wave Structures: A Special Form of Guided-Wave Structure," *IEEE Microw. Mag.*, vol. 14, pp. 87–96, 2013.
- [4] D.-F. Guan, Q. Zhang, P. You, Z.-B. Yang, Y. Zhou, and S.-W. Yong, "Scanning rate enhancement of leaky wave antennas using slow-wave substrate integrated waveguide (SIW) structure," *IEEE Trans. Antennas Propag.*, vol. 66, no. 7, pp. 3747–3751, Jul. 2018.
- [5] Y. Dong and T. Itoh, "Composite Right/Left-Handed Substrate Integrated Waveguide and Half Mode Substrate Integrated Waveguide Leaky-Wave Structures," *IEEE Trans. Antennas Propag.*, vol. 59, pp. 767–775, 2011.
- [6] D.-F. Guan, P. You, Q. Zhang, K. Xiao, and S. W. Yong, "Hybrid spoof surface plasmon polariton and substrate integrated waveguide transmission line and its application in filter," *IEEE Trans. Microw. Theory Techn.*, vol. 65, no. 12, pp. 4925–4932, Dec. 2017.
- [7] D.-F. Guan, P. You, Q. Zhang, Z.-B. Yang, H. Liu, and S.-W. Yong, "Slow-wave half-mode substrate integrated waveguide using spoof surface plasmon polariton structure," *IEEE Trans. Microw. Theory Techn.*, vol. 66, no. 6, pp. 2946–2952, Jun. 2018.
- [8] K. Chen, Y. Zhang, S. He, H. Chen, and G. Zhu, "A Novel Frequency Scanning Leaky-Wave Antenna Based on Corrugated Substrate Integrated Waveguide," *Int. J. Antennas Propag.*, vol. 2018, p. 6, 2018.
- [9] L. Chang, Y. Li, Z. Zhang, and Z. Feng, "Reconfigurable 2-Bit Fixed-Frequency Beam Steering Array Based on Microstrip Line," *IEEE Trans. Antennas Propag.*, vol. PP, p. 1–1, 2018.
- [10] Y. Li, M. F. Iskander, Z. Zhang, and Z. Feng, "A new low cost leaky wave coplanar waveguide continuous transverse stub antenna array using metamaterial-based phase shifters for beam steering," *IEEE Trans. Antennas Propag.*, vol. 61, no. 7, pp. 3511–3518, Jul. 2013.
- [11] R. Guzman-Quiros, J. L. Gomez-Tornero, A. R. Weily, and Y. J. Guo, "Electronic full-space scanning with 1-D Fabry-Pérot LWA using electromagnetic band-gap," *IEEE Antennas Wireless Propag. Lett.*, vol. 11, pp. 1426–1429, 2012.
- [12] S. Lim, C. Caloz and T. Itoh, "Metamaterial-based electronically controlled transmission-line structure as a novel leaky-wave antenna with tunable radiation angle and beamwidth," *IEEE Trans. Microw. Theory Techn.*, vol. 52, pp. 2678–2690, 2004.
- [13] J. H. Fu, A. Li, W. Chen, B. Lv, Z. Wang, P. Li, and Q. Wu, "An Electrically Controlled CRLH-Inspired Circularly Polarized Leaky-Wave Antenna," *IEEE Antennas Wireless Propag. Lett.*, vol. PP, p. 1–1, 2017.
- [14] A. Suntives and S. V. Hum, "A Fixed-Frequency Beam-Steerable Half-Mode Substrate Integrated Waveguide Leaky-Wave Antenna," *IEEE Trans. Antennas Propag.*, vol. 60, pp. 2540–2544, 2012.
- [15] A. Suntives and S. V. Hum, "An electronically tunable half-mode substrate integrated waveguide leaky-wave antenna," in *Proc. 5th EuCAP*, Apr. 2011, pp. 3670–3674.
- [16] K. W. Eccleston, "Mode Analysis of the Corrugated Substrate Integrated Waveguide," *IEEE Trans. Microw. Theory Techn.*, vol. 60, pp. 3004–3012, 2012.
- [17] Z. Liu, G. Xiao and L. Zhu, "Numerical de-embedding and experimental validation of propagation properties of corrugated substrate integrated waveguide," *Microw. Opt. Technol. Lett.*, vol. 58, pp. 2456–2460, 2016.
- [18] D. Deslandes and K. Wu, "Analysis and design of current probe transition from grounded coplanar to substrate integrated rectangular waveguides," *IEEE Trans. Microw. Theory Techn.*, vol. 53, pp. 2487–2494, 2005.